Original Paper

Sulfur chemistry in a borosilicate melt

Part 3. Iron-sulfur interactions and the amber chromophore[1])

Henry D. Schreiber, Samuel J. Kozak, Charlotte W. Schreiber, Douglas G. Wetmore, Margaret W. Riethmiller

Center for Glass Chemistry, Virginia Military Institute, Lexington, VA (USA)

The mutual interactions of iron and sulfur in a borosilicate melt were defined as a function of the iron content, sulfur concentration, melt temperature, and oxygen fugacity. Over the range of conditions for which ions of $SO_4^{2-}-Fe^{3+}-Fe^{2+}$ or $S^{2-}-Fe^{2+}-Fe^0$ existed in the melt, sulfur and iron behaved as two independent redox systems. Mutual interaction occurred only for the conditions when S^{2-} ions were in equilibrium with Fe^{3+} ions in the melt (for example, an oxygen fugacity of 10^{-9} to 10^{-11} bar at 1150 °C). The Fe^{3+} ion oxidized the S^{2-} ion to the supersulfide ion, S_2^-, which was identified as the amber chromophore. When the iron content of the melt was 1 wt% or less, the supersulfide ion was produced only in low concentrations; and consequently, the redox reaction producing it did not measurably affect sulfur solubility in the melt. In melts containing 10 wt% total iron, the mutual interaction of Fe^{3+} and S^{2-} ions was sufficient to enhance the sulfur solubility through the formation of polysulfide species in the melt.

Chemismus des Schwefels in einer Borosilicatschmelze

Teil 3. Eisen/Schwefel-Wechselwirkungen und der braune Farbträger

Die gegenseitigen Einwirkungen von Eisen und Schwefel in einer Borosilicatschmelze werden als Funktion des Eisengehaltes, der Schwefelkonzentration, der Schmelztemperatur und der Sauerstoffugazität beschrieben. Für die Verhältnisse, bei denen $SO_4^{2-}-Fe^{3+}-Fe^{2+}$ oder $S^{2-}-Fe^{2+}-Fe^0$ in der Schmelze existieren, verhalten sich Schwefel und Eisen wie zwei unabhängige Redoxsysteme. Eine gegenseitige Einwirkung tritt nur dann auf, wenn die S^{2-}-Ionen im Gleichgewicht mit Fe^{3+}-Ionen in der Schmelze stehen (z. B. bei einer Sauerstoffugazität von 10^{-9} bis 10^{-11} bar bei 1150 °C). Das Fe^{3+}-Ion oxidiert das S^{2-}-Ion zum Supersulfidion, S_2^-, das als der braune Farbträger (Kohlegelbträger) identifiziert wird. Bei einem Massenanteil von 1 % Eisen in der Schmelze oder weniger bildet sich das Supersulfidion nur in geringen Konzentrationen und deshalb beeinflußt die Redoxreaktion, die das Supersulfidion erzeugt, die Schwefellöslichkeit in der Schmelze nicht merklich. In Schmelzen mit einem Massenanteil von 10 % Gesamteisen reicht die Wechselwirkung zwischen den Fe^{3+}- und S^{2-}-Ionen in der Schmelze aus, um die Löslichkeit des Schwefels durch die Bildung von Polysulfidspezies zu erhöhen.

1. Introduction

1.1. Reference system

Savannah River Laboratory glass frit no. 131 (SRL-131) was used as a reference composition for this study; its composition (in wt%) is 57.9 SiO_2, 1.0 TiO_2, 0.5 ZrO_2, 14.7 B_2O_3, 0.5 La_2O_3, 2.0 MgO, 5.7 Li_2O, and 17.7 Na_2O [1]. This composition has been previously used to characterize sulfur redox chemistry and solubility [2] as well as sulfur transport properties [3] in borosilicate melts. SRL-131 glass melts have also been employed to define an electrochemical series of redox couples [4 and 5] and to compare the solubilities and diffusivities of various gases [6 and 7] in borosilicate solvents. The chemistry determined in SRL-131 has been shown to be applicable to a variety of other glass melts [8 to 11].

Received 24 February 1989, revised manuscript 2 January 1990.

[1]) Schreiber, H. D.; Kozak, S. J.; Leonhard, P. G. et al.: Sulfur chemistry in a borosilicate melt. Part 1. Redox equilibria and solubility. Glastech. Ber. **60** (1987) no. 12, p. 389–398. Part 2. Kinetic properties. Glastech. Ber. **61** (1988) no. 1, p. 5–11.

1.2. Sulfur chemistry in the reference glass melt

The solubility and redox chemistry of sulfur in SRL-131 glass melts are compiled in figure 1 [2]. The only redox states of sulfur incorporated in this borosilicate solvent at equilibrium are S^{6+} as the sulfate ion (SO_4^{2-}) and S^{2-}, the sulfide ion. Inter-

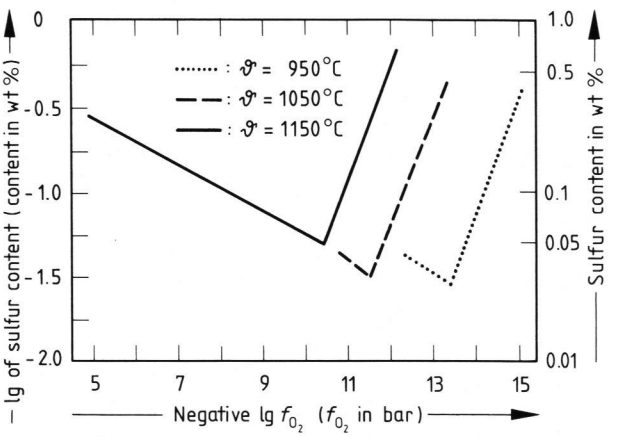

Figure 1. Solubility of sulfur in SRL-131 glass melts as a function of the imposed oxygen fugacity and glass melt temperature [2]. The SO_2 content of the atmosphere was kept constant at 15 vol%.

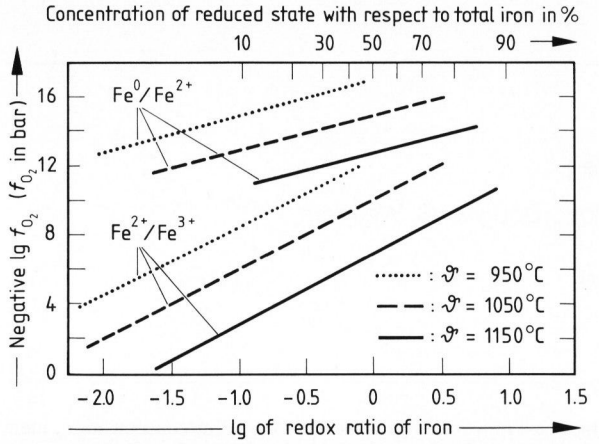

Figure 2. Relation of the imposed oxygen fugacity to the analyzed redox ratio of iron in SRL-131 glass melts containing 1 wt% iron at various glass melt temperatures.

mediate redox states, namely elemental sulfur or the sulfite ion, are not stable therein.

Sulfur solubility is intimately dependent on the redox state that is stabilized in the melt at a given oxygen fugacity. At 1150 °C sulfur dissolves exclusively as the sulfate ion at oxygen fugacities above 10^{-9} bar (oxidizing conditions), and exclusively as the sulfide ion at oxygen fugacities below 10^{-11} bar (reducing conditions). Only over a very narrow range of oxygen fugacities, between 10^{-9} and 10^{-11} bar at 1150 °C, do sulfate and sulfide ions coexist in the melt. This region also corresponds to a minimum in the solubility of sulfur [2 and 12]. The sulfate-sulfide equilibrium, and the corresponding sulfur solubility minimum, systematically shifts to more reducing conditions as the temperature decreases [2 and 12]. The sulfate ion solubility increases with decreasing temperature and increasing oxygen fugacity. On the other hand, the sulfide ion solubility in the melt increases with increasing temperature and decreasing oxygen fugacity.

Studies of the kinetic properties of sulfur in this reference melt [3] suggest that the diffusivities for both the sulfate ion and the sulfide ion are near identical. In addition, transient sulfur redox states in this glass were produced by placing an oxidized melt in a reduced sulfur atmosphere. Ions that are broadly categorized as polysulfide ions and radicals with respective formulas S_x^{2-} and S_y^- occur but slowly decay to the stable sulfide ions under these conditions.

An understanding of the chemistry of sulfur in the reference borosilicate system has many practical consequences. One example is the better understanding of sulfur compounds as fining agents for commercial glasses [2, 3, 7 and 11]. Another is that the reduction of sulfur to sulfide establishes a crucial lower limit (in terms of oxygen fugacity) for the operation of melters processing high-level nuclear waste [2, 10 and 13].

1.3. Redox chemistry of iron in the reference glass melt

Iron's redox chemistry has been extensively investigated in glass melts [14 and 15], in particular in this reference borosilicate glass [4, 8, 10, 16 and 17]. Iron may dissolve either as a mixture of Fe^{3+} and Fe^{2+} ions (oxidizing conditions) or as a mixture of Fe^{2+} and Fe^0 ions (reducing conditions). Since iron operates as a redox buffer in most glass melts because of its relatively high redox concentration and its central position in an electromotive force series [18 and 19], it generally controls the resulting redox state of the melt [9 and 10]. Figure 2 summarizes the redox chemistry of iron in SRL-131 melts [4, 8, 16 and 17]. The relative concentrations of Fe^{3+} and Fe^{2+} ions or of Fe^{2+} and Fe^0 ions are controlled principally by the imposed oxygen fugacity and the melt temperature. Low temperatures and high oxygen fugacities stabilize proportionally more ferric iron; high temperature and low oxygen fugacities can produce appreciable percentages of metallic iron; and intermediate conditions result in high relative concentrations of ferrous iron. The linear relationships between $-\lg f_{O_2}$ and lg of redox ratio in this figure are those predicted from equilibrium considerations {slope of 4 for $-\lg f_{O_2}$ versus lg ($[Fe^{2+}]/[Fe^{3+}]$), and slope of 2 for $-\lg f_{O_2}$ versus lg ($[Fe^0]/[Fe^{2+}]$)} [14 and 20]. The trends established in figure 2 are valid in other glass compositions as well [8 and 10].

Iron impurities in commercial glasses typically produce an unwanted color. Such color can either be controlled chemically by adjustment of the redox state of the glass melt or neutralized physically by additives to the batch [21]. In nuclear waste immobilization, the iron redox state is used as a monitor for processing control of the dissolution of the waste in the glass melt [10, 22 and 23]. Both cases show the need for an understanding of the redox chemistry of iron in glass melts.

1.4. Iron-sulfur interactions in glass melts

Iron and sulfur (with oxygen) are typically the crucial redox components of glasses. In most commercial glasses, iron is present as an impurity or a redox additive; while sulfur compounds are impurities, fining agents, or color additives. Iron is also a major constituent of high-level nuclear waste which is present as a sulfate sludge; thus, iron-sulfur interactions are of paramount importance during the processing of nuclear waste into a glass. Certain interactions of iron and sulfur in glass melts are well-established, albeit not well understood. Amber glass containing both iron and sulfur is used as container glass for the protection of foodstuffs, beverages, and chemicals from ultraviolet light [21 and 24]. In other glasses, the presence of iron is known to enhance the solubility of sulfur [12, 25 to 27].

1.5. Amber chromophore in iron-sulfur glasses

Amber (golden-yellow) coloration is produced in silicate glasses melted with small quantities of iron and sulfur under reducing conditions. Empirical rules govern the generation of this color in glass. The total iron content is between 0.1 and 0.2 wt% (although as little as 0.0006 wt% can be used), while the intensity of the amber is controlled by varying the sulfur content [21, 24 and 28]. Carbon additions to the batch regulate the redox conditions which must be reducing enough to stabilize the sulfide ion, but yet sufficiently oxidizing for some iron to be in the Fe^{3+} state [21 and 24]. Good amber coloration in soda-lime-silica glasses requires an oxygen fugacity between 10^{-8} and 10^{-10} bar [21]. Figure 3 and table 1 illustrate some properties of amber glass for two typical samples. An absorption peak at about 400 nm is characteristic of these glasses. Increasing the total amount of iron and sulfur in the glass enhances this absorption peak and, thus, the amber color. For both samples, 75 % of the sulfur is present as sulfide and about 25 % of the iron is ferric [21, 29 to 31]. Figures 1 and 2 for SRL-131 glass show that the range of oxygen fugacities under which the sulfide and ferric ions could coexist is relatively narrow, about 10^{-8} to 10^{-10} bar, which also corresponds to the minimum in sulfur solubility.

The amber chromophore, the chemical species responsible for the color or for the absorption peak at 400 nm, is widely attributed to an iron-sulfur complex in the glass [21, 24, 32 to 35]. In many iron-containing glasses, the Fe^{3+} ion is tetrahedrally coordinated to four oxide ions. The amber chromophore supposedly forms when a sulfide ion replaces one of these oxides in the Fe^{3+} coordination sphere [24, 32 and 33]. Electronic charge-transfer between the central ferric ion and the sulfide ligand causes an intense absorption at 400 nm (the exact wavelength is dependent on the glass composition) [21, 33 to 35], which allows only the yellow-red light to be transmitted. The chromophore is present in the glass in relatively low concentration, as only 12 to 15 % of all the Fe^{3+} ion and 5 to 7 % of all S^{2-} ion participate in the iron-sulfur complex [34]. The ferric iron signal in Electron Paramagnetic Resonance (EPR) spectroscopy is consistent with the Fe^{3+} ion being perturbed by one sulfide ion in its coordination sphere in amber glass [36 and 37].

Amber coloration has been assumed to require both iron and sulfur, resulting in the identification of an iron-sulfur chromophore [21]. However, others have attributed the coloration to $Fe^{2+}-S^{2-}$ color centers [38], or to polysulfide ions formed by the interaction of sulfur with the iron [28]. An intense amber color was attained in the iron-free SRL-131 glass, albeit as a transient species; this coloration was credited to the formation of polysulfide ions or radicals [3].

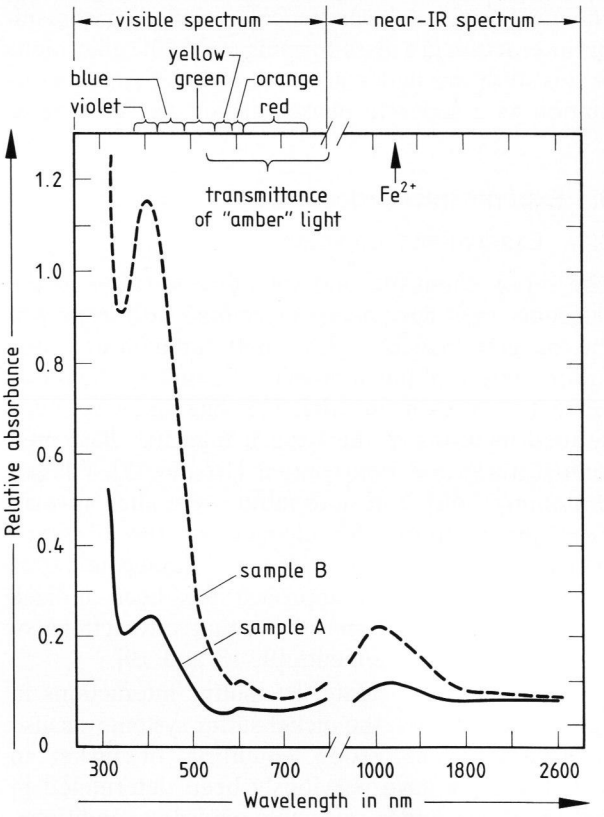

Figure 3. Visible and near-infrared spectra of two samples of amber glass with a glass thickness of 1.5 mm. Sample A is a light amber glass distributed by Technical Committee 14 of the International Commission on Glass as a possible standard glass. Sample B is a typical dark amber bottle glass. Iron and sulfur analyses of these samples are provided in table 1.

2. Objectives

The objectives of this study are to ascertain first the effect of iron on the solubility and redox states of sulfur in the reference borosilicate glass melt, second the effect of dissolved sulfur on the iron redox distribution in the reference system, and third the identity and amounts of the products of iron-sulfur interactions. Of particular concern is understanding the

Table 1. Redox analyses of typical amber glasses. Glasses A and B are as described in figure 3

glass	color	total sulfur content in wt%	S^{2-} content in wt%	total iron content in wt%	Fe^{2+} content in wt%
A	light amber	0.008 ± 0.002	0.006 ± 0.002	0.053 ± 0.007	0.040 ± 0.005
B	dark amber	0.03 ± 0.01	0.02 ± 0.01	0.23 ± 0.02	0.18 ± 0.02

chemical origin of the amber coloration as an iron-sulfur interaction in a glass-forming melt. The glass melts in this study are undersaturated with FeS; and its formation as a separate phase will not be considered.

3. Experimental procedures

3.1. Experimental approach

The redox chemistry and solubility of sulfur in the reference melt have been determined with respect to the oxygen fugacity, glass melt temperature, and sulfur content of the atmosphere [2 and 3]; the redox behavior of iron in SRL-131 has likewise been defined in terms of the oxygen fugacity, glass melt temperature, and iron content [16 and 17]. Glasses containing both iron and sulfur were then investigated to monitor any changes in the observed properties caused by the addition of the second redox component. Such an approach has been utilized previously to ascertain the mutual interactions of other multivalent elements [9, 18 and 19].

In order to elucidate iron-sulfur interactions in this reference glass, the nickel-sulfur system was also investigated. The redox equilibria of nickel in SRL-131 glass have previously been determined [4 and 16]. Even under extremely oxidizing conditions, only a small fraction of nickel occurs in the Ni^{3+} state; nickel metal precipitates under reducing conditions; and the Ni^{2+} ion is stable over a wide range of oxygen fugacities.

3.2. Base composition

Bulk glasses of the SRL-131 base composition containing a specified quantity of iron (or nickel) were prepared by weighing known quantities of SRL-131 frit and Fe_2O_3 (or NiO), mixing the powders, melting in a platinum crucible above 1000 °C for at least 18 h, rapid quenching into water, and powdering in an alumina mortar and pestle. Nominal concentrations of iron (or nickel) in these glasses were prepared to be 0.1, 1, and 10 wt% iron (or 1 wt% nickel). Sulfur was not included in these batches but was introduced by bringing individual samples to equilibrium in sulfur-containing atmospheres.

3.3. Sample syntheses

Rings of about 4 to 5 mm in diameter were fabricated from 0.5 mm platinum-rhodium wire. About 0.35 g of the powdered glass was sintered onto the platinum ring by placing the ring and powder in a concave graphite crucible at about 1000 °C for a few minutes [2]. The glass did not wet the surface of the graphite, but did adhere to the inert metal ring forming a spherical bead.

Individual samples were then placed in a high-temperature, vertical-tube furnace with precision thermal and atmospheric control [2 and 3]. The platinum ring containing the glass was suspended in the hot zone of the furnace, the molten glass being retained on the ring by its surface tension [2 and 39]. This technique was employed to minimize the time needed for equilibration with the atmosphere (by maximizing the exposed surface area) as well as to minimize iron loss from the glass melt into the container [39]. The actual temperature of the sample was controlled within ± 2 K, and was monitored by a $Pt/Pt_{90}Rh_{10}$ thermocouple. Atmospheric control of partial pressures of O_2 and SO_2 at 1.01 bar total pressure was obtained by mixing CO_2, CO, and SO_2 [2 and 12]. Individual samples were equilibrated for about 4 h; kinetic studies had shown that this was sufficient to achieve equilibrium [2 and 3].

Series of samples were synthesized for each composition at several glass melt temperatures (1150, 1050, or 950 °C) in an atmosphere containing 5 or 15 vol% of SO_2 over a wide range of imposed oxygen fugacities. Several series were duplicated to confirm the reproducibility of the results.

3.4. Spectrophotometry for sample analyses

Individual samples were mounted in acrylic from which sections of glass were obtained. Approximate dimensions of the sections were 4 to 5 mm in diameter and from 0.1 to 2 mm in thickness. Microscopic analyses ascertained the color and homogeneity.

Near-infrared spectra (2600 to 800 nm) on the polished slabs were obtained on a Beckman 5240 spectrophotometer (Beckman Instrument Co., Fullerton, CA (USA)). As shown in figure 3, the only features observed in this region for the iron-sulfur samples were a peak at 1000 nm and a weak shoulder at 1880 nm. Both are attributable to the Fe^{2+} ion in the glass [17 to 19]. The absorptivity index (defined as the peak minus baseline absorbance per unit thickness) of the peak at 1000 nm for each sample was determined, since it had previously been calibrated to Fe^{2+} concentration [18 and 19]. For samples synthesized at the lowest oxygen fugacities, background from the visible region overwhelmed the weak Fe^{2+} peak at 1000 nm, resulting in low accuracy analyses.

Visible spectra (800 to 300 nm) on the polished slabs were also obtained on a Beckman 5240 spectrophotometer. The characteristic absorbances of amber glass at 410 nm as well as at 630 nm, as illustrated in figures 3 and 4, were monitored in terms of their absorptivity indices. The ultraviolet absorption edge is probably controlled by iron (Fe^{3+}) charge transfer transitions for glasses synthesized under oxidizing conditions [40], and by sulfide ion absorptions for glasses synthesized under reducing conditions [2]. The minor, but sharp, absorbances in the spectra are due to neodymium impurities in the SRL-131 glass. In nickel-containing glasses, the Ni^{2+}

ion displayed absorbances at 445 and 645 nm. Absorptivity indices of the 445 nm peak were used to determine Ni^{2+} concentrations in the glasses [16]. The absence of the amber absorbance in the nickel-doped glasses allowed the sulfide content of the glass to be estimated by measuring the absorbances at set points on the ultraviolet absorption edge [2 and 3]. After spectral analyses, each polished slab and any remaining portion of that sample were finely powdered.

3.5. Magnetic susceptibility and determination of iron

About 0.2 g of each sample powder was analyzed with a magnetic susceptibility balance (Johnson Matthey Inc., Wayne, PA (USA)). The presence of iron or nickel metal in the glass samples was monitored by enhanced magnetic susceptibilities.

Nominal concentrations of total iron in the glasses were calculated from the weighed quantities of iron and SRL-131 glass. The Fe^{2+} contents were determined from the calibrated near-infrared absorption at 1000 nm. This analysis was best when the Fe^{2+} ion coexisted with Fe^{3+} ion rather than with Fe^0 ion. A 10 to 20 mg aliquot of glass powder was dissolved in acid in an argon atmosphere. After proper buffering of the solution, an o-phenanthroline solution was added forming a characteristic red complex with the Fe^{2+} ion from the dissolved glass [41]. This complex possessed an intense absorbance at 510 nm, which was calibrated to Fe^{2+} concentration by using standard solutions of known iron contents. Additions of hydroquinone then reduced all iron to the Fe^{2+} state. Reanalysis of the 510 nm absorbance of the o-phenanthroline complex measured the total iron content. These total iron analyses usually agreed with the nominal iron concentrations to within ± 7 %.

3.6. Sulfur determination

100 to 150 mg aliquots of the glass powders were analyzed for total sulfur concentrations [2]. Each sample was digested in a mixture of acid and reducing agents so that all sulfur in the glass was reduced to the sulfide ion. In particular, the treatment evolved H_2S which was distilled and collected in a standard anti-oxidizing buffer. The sulfide content of this solution, as determined by a calibrated specific ion electrode, reflected the total sulfur content in the original sample.

For a series of samples prepared at constant iron content, temperature, and atmospheric sulfur content as a function of the imposed oxygen fugacity, the presence of the analyzed sulfur as sulfate or as sulfide was assigned by being to the left or to the right, respectively, of the sulfur solubility minimum, in accordance with figure 1. Other methods to analyze specifically for the concentration of the sulfide ion in glasses containing both iron and sulfur rely on redox titrations to analyze the total reducing ion concentration ($Fe^{2+} + S^{2-}$) and on spectrophotometric procedures to ascertain the Fe^{2+} content [29]. Sulfide concentration is then calculated from the difference. When samples were analyzed in this fashion, they established that the sulfur on the low oxygen fugacity side of the solubility minimum was indeed the S^{2-} ion and on the high oxygen fugacity side was void of the S^{2-} ion.

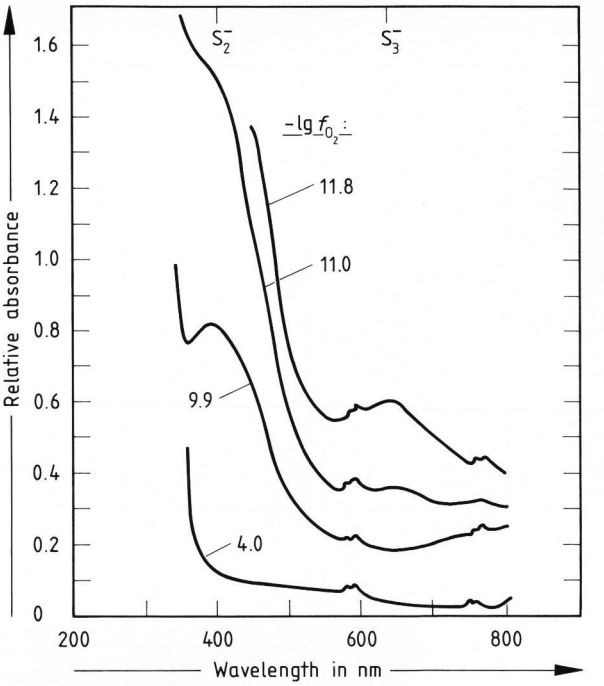

Figure 4. Visible spectra of SRL-131 glasses containing 1 wt% iron with a glass thickness of 1.2 to 2.1 mm. Glasses were synthesized at 1150 °C, 15 vol% SO_2 in the atmosphere, and various oxygen fugacities.

4. Results

4.1. Spectroscopic characterization of iron-sulfur glasses

Spectral characteristics of Fe-S glasses in the reference glass containing 1 wt% total iron are summarized in figure 4. The spectra of oxidized glasses possessed only an ultraviolet absorption edge originating from charge transfer transitions between the iron species [40]. For glasses prepared below an oxygen fugacity of 10^{-9} bar at 1150 °C, an absorption peak developed at about 400 nm. Under steadily decreasing oxygen fugacities, this absorbance at 400 nm systematically increased. This peak eventually was incorporated into the ultraviolet absorption edge at a sufficiently low oxygen fugacity, while a relatively weak absorbance at 630 nm developed. This ultraviolet absorption edge is associated with the stabilization of the sulfide ion in the reduced glasses [2]. Amber colorations of the glasses corresponded to the appearance of a discrete 400 nm absorption,

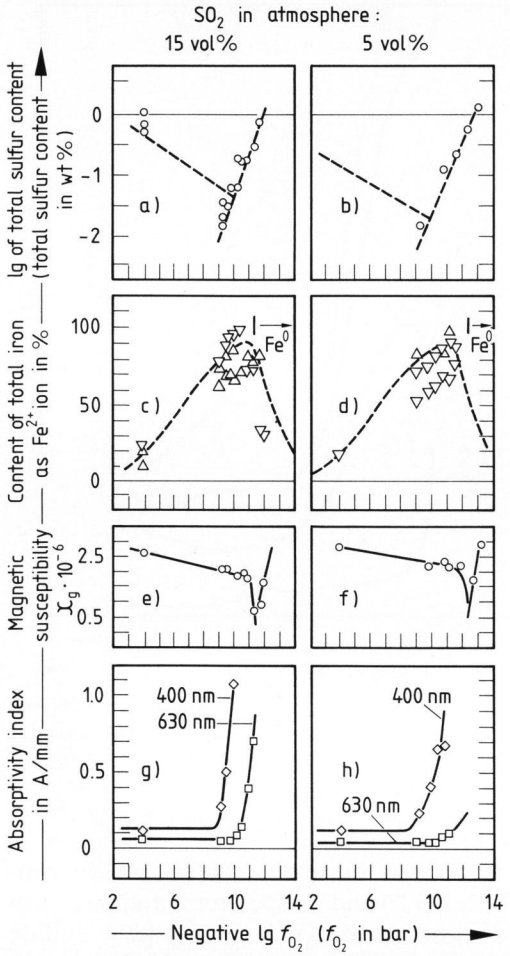

Figures 5a to h. Chemical and spectral characterization of SRL-131 glasses containing both iron (1 wt%) and sulfur at 1150 °C. The solubility of sulfur, the iron redox distribution, the magnetic susceptibility and the absorptivity indices of the amber chromophore are reported as a function of the imposed oxygen fugacity for 5 and 15 vol% SO_2 in the atmosphere. The dashed lines for the sulfur solubility refer to an iron-free SRL-131 glass melt, while the symbols (○) refer to the experimental solubility melts containing 1 wt% total iron (figures 5a and b). The dashed lines in the iron redox distributions refer to distributions in a SRL-131 glass melt not containing sulfur, while the symbols (△) refer to iron redox distributions measured in melts exposed to the sulfur atmosphere (figures 5c and d). The symbols (△) report results from o-phenanthroline analyses, whereas the symbols (▽) use nominal iron concentrations and spectrophotometric analyses of Fe^{2+} contents. Magnetic susceptibility monitors iron metal precipitation (figures 5e and f). Absorptivity indices at 400 nm (diamonds) and at 630 nm (squares) relate to the concentration of the amber chromophore (figures 5g and h).

which was observed in glasses prepared between 10^{-9} and 10^{-11} bar at 1150 °C. Glasses containing 10 wt% iron were essentially black and did not change color with sulfur additions.

4.2. Variation in atmospheric sulfur content

Figures 5a to h summarize the results for two series of glasses prepared at 1150 °C in SRL-131 glass containing 1 wt% total iron. These series investigated the properties of iron-sulfur glasses synthesized at different atmospheric SO_2 contents as a function of the imposed oxygen fugacity.

Little if any effect of sulfur on the iron redox distribution in the glass melts was observed. Likewise, little if any effect of iron (at the 1 wt% level) on the sulfur solubility was identifiable. The iron redox distribution can therefore be independently combined with the sulfur redox/solubility relations to define a region of Fe^{3+} and S^{2-} coexistence in SRL-131 glass between 10^{-9} and 10^{-11} bar at 1150 °C. Under more oxidizing conditions, sulfate ions coexist with the Fe^{3+}/Fe^{2+} redox couple; whereas under more reducing conditions, sulfide ions are in equilibrium with Fe^{2+} ions and precipitating iron metal.

Absorptions in the visible spectra of iron-sulfur glasses correlate with the appearance of amber coloration. However, the lack of perturbation in the individual solubility and redox relations implies that the iron-sulfur mutual interaction (the amber chromophore) involves only a small concentration of contributing units. The intensity of the absorbances at a given oxygen fugacity is proportional to the atmospheric SO_2 content, indicative that sulfur is an active component of the chromophore.

The initial appearance of the 400 nm absorbance, as the oxygen fugacity is systematically lowered, corresponds to the stabilization of appreciable quantities of sulfide in the glass. This limit is dependent only on the imposed oxygen fugacity (10^{-9} bar at 1150 °C) and not on the prevailing SO_2 content of the atmosphere. As the oxygen fugacity is lowered, the 400 nm absorbance steadily increases in intensity until it becomes a part of the ultraviolet absorption edge (figure 4). Although the apparent absorptivity index at 400 nm continues to increase with decreasing oxygen fugacity, the peak is no longer resolvable as a discrete entity. The 630 nm absorbance peak appears only at more reducing conditions than that stabilizing the 400 nm peak. Its occurrence is not dependent on the SO_2 content of the atmosphere; but the peak intensity at a particular oxygen fugacity is indeed dependent on the atmospheric SO_2 percentage. The 630 nm absorbance corresponds to the region where sulfur is exclusively incorporated as sulfide in the melt. Amber colorations in the iron-sulfur glasses result from the 400 nm absorption in the glass, but the distinctive color dissipates at low oxygen fugacities when the peak becomes a part of the absorption edge. The amber coloration correlates to the coexistence of sulfide and ferric ions in the melt (between 10^{-9} and 10^{-11} bar at 1150 °C).

Figures 5a to h show firstly that iron and sulfur only interact in the melt when iron is present as Fe^{3+} ion and when sulfur is present as S^{2-} ion; secondly that the stability of the amber chromophore depends on the coexistence of Fe^{3+} and S^{2-} ions; thirdly that the amber intensity is principally controlled by the amount of sulfur as sulfide (and not by the amount of

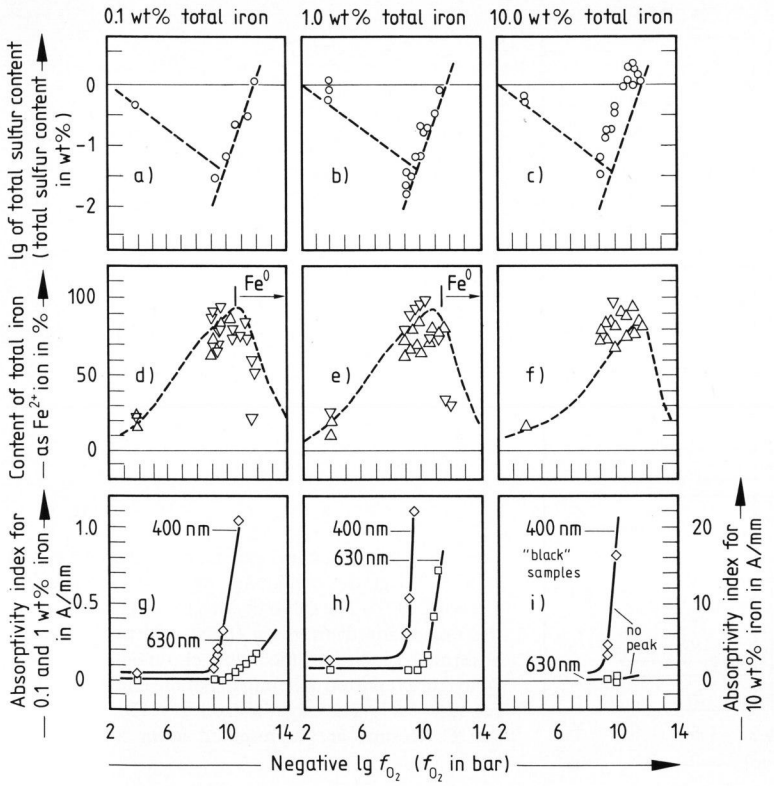

Figures 6a to i. Chemical and spectral characterization of SRL-131 glasses containing iron and sulfur (15 vol% in atmosphere) at 1150 °C. The solubility of sulfur (figures 6a to c), the iron redox distribution (figures 6d to f), and the absorptivity indices of the amber chromophore (figures 6g to i) are reported as a function of the imposed oxygen fugacity for three different iron contents of the melt (0.1, 1, and 10 wt%). Results are represented as in figures 5a to h.

iron as the ferric ion); and fourthly that only a relatively small percentage of the iron and sulfur is responsible for the amber chromophore.

4.3. Variation in iron content of the glass melt

Iron and sulfur properties are compared in figures 6a to i for 0.1 wt% versus 1.0 wt% total iron in SRL-131 glass melt. In addition to the results of the prior section being supported, the concentration of the amber chromophore as monitored by the intensity of the 400 nm absorbance is shown to be proportional to the iron content. Thus, not only is the concentration of the chromophore proportional to the total sulfur concentration (or S^{2-} ion) but also to the total iron concentration (or Fe^{3+} ion). The amount of iron, as long as it is less than 1 wt%, does not affect the stability region of the amber chromophore. The occurrence is still determined solely by the prevailing oxygen fugacity, and not the iron or sulfur content. Furthermore, the intensity of the 630 nm absorbance is also proportional to both sulfur and iron concentrations, although its presence does not correlate with the amber coloration in the glass. The stabilization of this absorbance is likewise dependent only on the oxygen fugacity.

SRL-131 glass with 10 wt% total iron is colored black. Such glasses do not possess a discrete absorbance at 400 nm but have a high background absorption whose low wavelength absorptivity edge steadily creeps into the visible region as the synthesis conditions become more reducing. No precipitation of sulfur-rich phases from the borosilicate melt was observed. The presence of 10 wt% total iron in the melt did affect the sulfur solubility, albeit only over a narrow range of oxygen fugacities as shown in figures 6a to i. From an oxygen fugacity of 10^{-9} bar to that of 10^{-11} bar at 1150 °C, the sulfur solubility is greatly enhanced. This is the same range of oxygen fugacities as for the stabilization of the amber chromophore in SRL-131 glass containing 1 wt% or less total iron. The excess of sulfur is dissolved as a sulfide-like ion, since the solubility of sulfur as a function of the imposed oxygen fugacity is parallel to the sulfide solubility relationship in the absence of iron. Concurrent with the perturbation in the sulfur solubility is a systematic variation of the iron redox distribution. The glass melt possessed proportionally more Fe^{2+} ions at the expense of Fe^{3+} ions over this range of oxygen fugacities. The iron-sulfur interaction is not just a simple compositional dependence of the sulfur solubility, because it exists only over the narrow range of oxygen fugacities. The Fe^{3+} ion is probably being reduced by the large excess of S^{2-} ions. The sulfide ion is oxidized but not to the sulfate ion. Elemental sulfur was not observed in these glasses. The mechanism for enhanced sulfur solubility may be analogous to that which results in amber coloration for glasses with less iron.

4.4. Variation in glass melt temperature

Series of samples which contained a constant amount of iron (1 wt%) in SRL-131 glasses and were

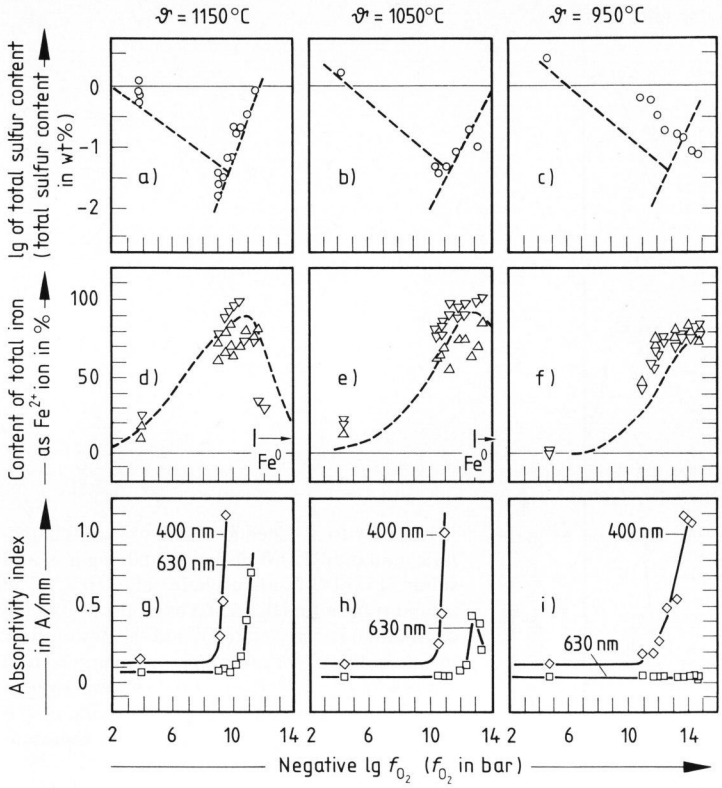

Figures 7a to i. Chemical and spectral characterization of SRL-131 glasses containing iron (1 wt%) and sulfur (15 vol% SO_2). The solubility of sulfur (figures 7a to c), the iron redox distribution (figures 7d to f), and the absorptivity indices of the amber chromophore (figures 7g to i) are reported as a function of the imposed oxygen fugacity for glasses synthesized at 1150, 1050, and 950 °C. Results are represented as in figures 5a to h.

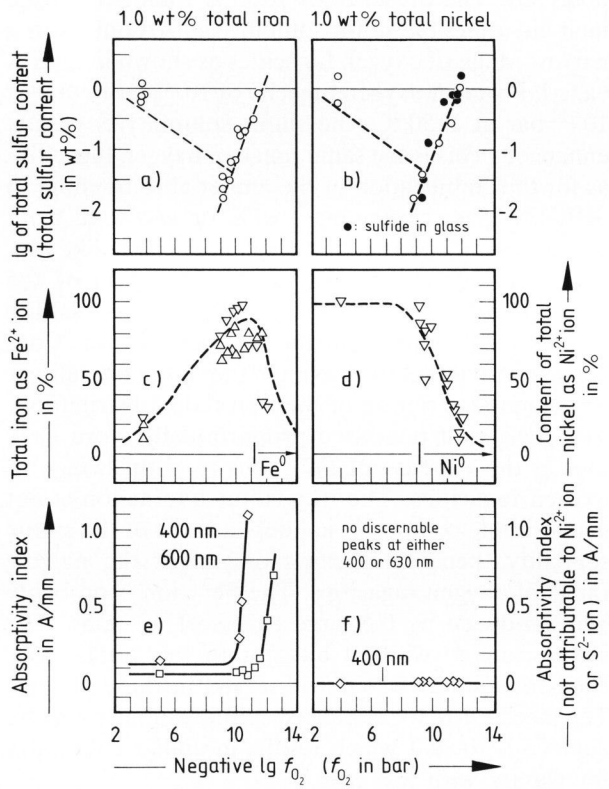

Figures 8a to f. Chemical and spectral characterization of SRL-131 glasses containing a transition metal and sulfur (15 vol% SO_2) at 1150 °C. The solubility of sulfur (figures 8a and b), the redox distribution of iron or nickel (figures 8c and d), and the absorptivity indices of the amber chromophore (figures 8e and f) are reported as a function of the imposed oxygen fugacity for glasses containing either iron (1 wt%) or nickel (1 wt%).

synthesized at a constant SO_2 percentage (15 vol%) are reported as a function of the oxygen fugacity for three melt temperatures in figures 7a to i. Once again, little if any mutual interaction of iron with sulfur is measured by variations in their redox and/or solubility relations with oxygen fugacity. The solubility of sulfur at 950 °C deviates from the trend because of an immiscible sulfate phase in equilibrium with the borosilicate glass melt [11].

The amber chromophore is again correlated to the oxygen fugacities where the sulfide ions and ferric ions coexist. As the region of $Fe^{3+}-S^{2-}$ coexistence shifts to lower oxygen fugacities with decreasing temperatures, the stabilization of the amber chromophore as monitored by the 400 nm peak shifts to lower oxygen fugacities. The amber chromophore is stabilized by high temperatures. For the same amount of Fe^{3+} and S^{2-} ions at a lower temperature, the intensity of the peak (as well as the color) is decreased. The intensity of the 630 nm peak is also drastically affected by temperature. At 950 °C the species responsible for this absorbance is no longer viable.

4.5. Variation in transition metal in the glass melt

Figures 8a to f illustrate the effect of nickel substituting for iron at the 1 wt% level. The presence of nickel does not alter the solubility or redox of sulfur in the glass melt; and likewise, the presence of sulfur

does not alter the nickel redox relations. No spectral absorbances in the visible or near-infrared region were attributable to nickel-sulfur interactions in these glasses. In particular, no evidence of a nickel-sulfur amber chromophore was found.

4.6. Summary of results

Iron and sulfur do not interact in the reference glass melt at oxygen fugacities more oxidizing than 10^{-9} bar or at oxygen fugacities more reducing than 10^{-11} bar (at 1150 °C). There is also no interaction between nickel and sulfur. Iron and sulfur will interact in glass melts over the range of oxygen fugacities where Fe^{3+} and S^{2-} ions coexist. The mutual interaction results in a product, the amber chromophore, that absorbs at 400 nm. The concentration of the amber chromophore increases as the iron or sulfur concentration increases. However, the concentration of the amber chromophore is more sensitive to the sulfide ion, since the intensity of the amber absorption increases rapidly as the amount of sulfide ion increases. The concentration of the amber chromophore in the glass is very low, as only small quantities of ferric ions and sulfide ions participate in its formation – so small that the sulfur and iron redox relations are not perturbed. The chromophore is stabilized by high temperatures. A secondary absorbance at 630 nm behaves similarly but occurs at lower oxygen fugacities when all sulfur is present as sulfide. Its intensity is always much less than the 400 nm peak.

When large concentrations of iron are present, iron-sulfur interactions also occur only between oxygen fugacities of 10^{-9} and 10^{-11} bar (at 1150 °C), the region where Fe^{3+} and S^{2-} ions coexist. However, in this case the sulfide solubility is enhanced by about an order of magnitude, and some ferric iron is reduced to ferrous iron. This interaction may be a combination of two mechanisms: one related to amber chromophore formation, and the second a compositional effect due to the large quantities of iron present.

5. Discussion

5.1. Glass melt conditions for iron-sulfur interactions

Conditions necessary for the interaction of iron and sulfur redox states are not dependent on the iron or sulfur content of the glass melt. Conditions are determined entirely by the oxygen fugacity and the temperature. Iron and sulfur function as two separate entities over most melt conditions within the reference glass, in that sulfate solubility is not perturbed by the Fe^{3+}/Fe^{2+} redox couple and sulfide solubility is not affected by the Fe^{2+}/Fe^{0} redox couple. However, there is a narrow range of oxygen fugacities for which Fe^{3+} ions coexist and interact with S^{2-} ions to form the amber chromophore. In the reference glass melt at 1150 °C, this oxygen fugacity range is from 10^{-9} to 10^{-11} bar; while in commercial amber glass compositions, the range is usually reported as 10^{-8} to 10^{-10} bar [21, 32, 33 and 37].

5.2. Magnitude and type of iron-sulfur interactions in the glass melt

The magnitude of iron-sulfur interactions depends on the iron and sulfur content. These interactions can be divided into two categories depending on the iron content of the glass.

For low concentrations of iron (1 wt% or less) in the glass, the interaction is limited to the production of the amber chromophore. The amount of the chromophore is controlled by the Fe^{3+} and S^{2-} concentrations, but the S^{2-} contents have the greater effect. However, since there is no mutual perturbation of the iron redox distribution or sulfur solubility, the actual concentration of the chromophore in the glass is quite low.

For relatively high concentrations of iron (10 wt%), the interaction is more dramatic. Over the range of $Fe^{3+}-S^{2-}$ coexistence, the sulfur solubility is enhanced by almost an order of magnitude and the iron redox distribution is shifted to produce about 10 % more Fe^{2+} ions. The Fe^{3+} ion oxidizes some of the S^{2-} ions to a S^{2-}-like ion but with greater solubility.

5.3. Amber chromophore

Studies [33, 35 and 37] have argued that the absorption peak at 400 nm in amber glasses is indeed the result of iron-sulfur interactions, and cannot be attributed to just iron or just sulfur. Accordingly, the amber chromophore was identified as a Fe^{3+} ion whose coordination sphere included one S^{2-} ion in addition to three oxide ions [21, 24, 29, 32, 36 and 37]. However, the amber chromophore has also been observed in an iron-free glass [3]. Although the chromophore in this case is produced as a transient species by the reaction of sulfide ions with excess oxygen, the product duplicates the spectral features and the color. The chromophore should be perceived as a sulfur species more oxidized than the S^{2-} ion, but yet not sulfate, sulfite, or elemental sulfur. In addition, this chromophore is only stable as long as the oxidizing agent (Fe^{3+} ion or O_2) remains in excess in the glass melt.

Glasses colored from red to blue have been produced from sulfur-containing alkali borate glass melts [42 to 45]: Such glasses are characterized by absorbance peaks at about 400 and 600 nm, with the intensity ratio determining the resulting color. For example, if the intensity of the 400 nm peak is greater

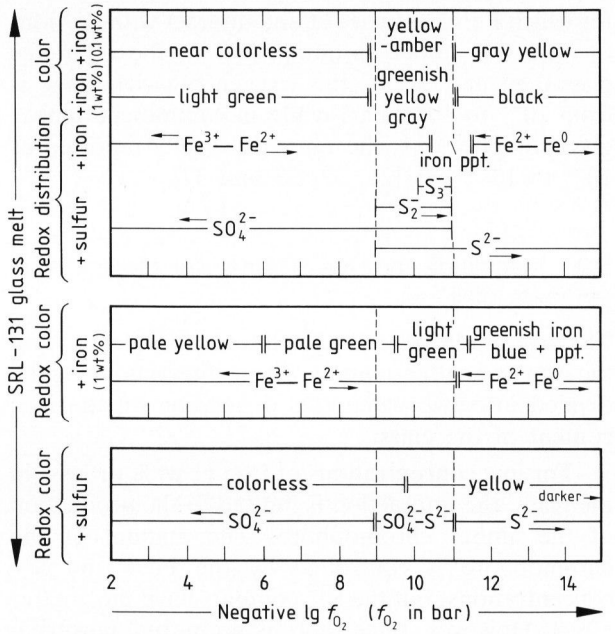

Figure 9. Redox and color identifications of glasses synthesized at a glass melt temperature of 1150 °C in SRL-131 glass melt containing just iron, just sulfur, or iron and sulfur simultaneously as a function of the imposed oxygen fugacity.

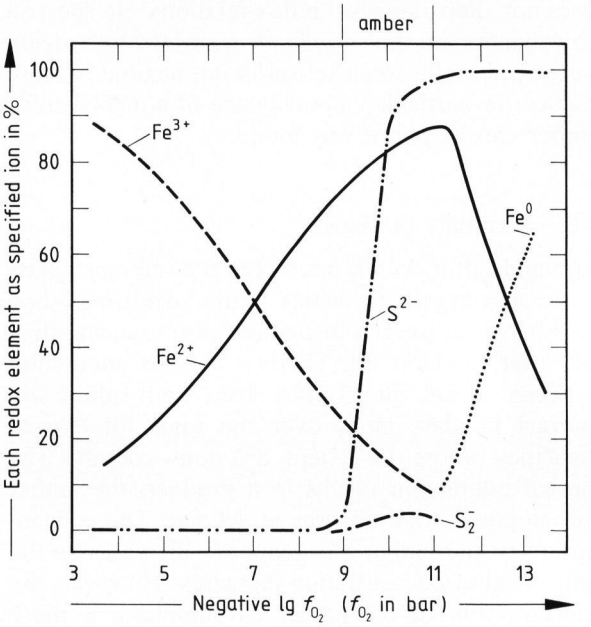

Figure 10. Distribution of iron and sulfur redox states in SRL-131 glass melt containing 1 wt% iron and synthesized in an atmosphere containing 15 vol% SO_2 at 1150 °C. The percentage sulfur as the sulfate ion is the difference of sulfur as S^{2-} and S_2^- ion from 100.

than that of the 600 nm peak, the color of the glass is red [42 to 44]. The 400 nm absorbance is due to the presence of S_2^- ions; and the 600 nm absorbance is attributed to S_3^- ions in the glass [42 to 44]. Such identifications and correlations are also valid in other melt systems [45 and 46] and in nonaqueous solvents [47 to 49].

Thus, the amber chromophore in the reference system (and in other base compositions) can by analogy be identified as the supersulfide ion, S_2^-, which is formed by the oxidation of the sulfide ion;

$$3\,Fe^{3+} + 2\,S^{2-} \rightleftharpoons 3\,Fe^{2+} + S_2^- \qquad (1)$$

in iron-containing glass melts, or

$$3\,O_2 + 8\,S^{2-} \rightleftharpoons 6\,O^{2-} + 4\,S_2^- \qquad (2)$$

in melts containing excess oxygen. As the concentration of the supersulfide ion increases, disproportionation of this product occurs;

$$4\,S_2^- \rightleftharpoons 2\,S_3^- + S_2^{2-} \qquad (3)$$

where the S_3^- ion is the thiozonide ion and is responsible for the 630 nm absorption in the reference system, and the S_2^{2-} ion is a polysulfide species contributing to additional absorptions at 400 nm and the ultraviolet absorption edge [44 and 47]. The concentration of the thiozonide ion is never greater than 10 % of that of the supersulfide ion in inorganic melts [45], in agreement with the results in SRL-131 glass melts. Figure 9 compiles the identifications of ions responsible for the glass colors, as well as their stability ranges with respect to oxygen fugacity for the reference system.

The molar absorptivity of the supersulfide ion at 400 nm is estimated to be 2400 l/(mol cm) in dimethylformamide [47], 4600 l/(mol cm) in chloride melts [47], and 2300 l/(mol cm) in potassium thiocyanate glass melts [45] – compared to a value of 9000 l/(mol cm) of the 400 nm peak in amber sodium silicate glass [29 and 34]. For amber glass in the reference system, the supersulfide ion concentration is estimated to be 0.002 wt% from these molar absorptivities. Consequently, the percentage of the sulfur actually present as the S_2^- ion in amber glass is just a fraction of the sulfur present as the S^{2-} ion, typically about 1 to 6 %.

The supersulfide ion is probably located at non-bridging oxygen sites within the melt. This is consistent with the compositional dependency of the amber chromophore, which is correlated to the availability of non-bridging oxygens [24, 34 and 44]. Since an "oxide" ion is replaced by a singly charged supersulfide ion in this mechanism, charge neutralization requires the S_2^- ion to be coupled to the Fe^{3+} ion. Thus, the purpose of the ferric ion in the melt is twofold – to oxidize the sulfide ion to the chromophore, and then to stabilize the resulting ion in the glass network. EPR evidence is consistent with this assignment, as it requires a perturbed Fe^{3+} site for the amber chromophore.

If 75 % of the sulfur in amber glass is initially present as S^{2-} ion (of which 5 % actively participates

in the chromophore production) and 20 % of the iron in amber glass is initially present as Fe^{3+} ion (of which 12 % actively participates in the chromophore production) [28 to 31 and 34], then only 2 % of all the iron and 4 % of all the sulfur in the glass melt are affiliated with the amber chromophore. These amounts are not sufficient to cause deviations in the observed iron redox distributions and sulfur solubilities. This also provides an estimate of the supersulfide concentration in the melt identical to that predicted from the molar absorptivities. The amount of S_2^- ions in amber glass with respect to the other iron and sulfur redox states is illustrated in figure 10. The S_3^- concentration is negligible. The thermal dependence of the supersulfide ion is also consistent with the results of this study, as it is stabilized by high temperatures [45].

5.4. Solubility enhancement of sulfur in iron-rich glass melts

This study as well as others [25, 27 and 50] have shown that high concentrations of iron enhance the capacity of the glass melt to dissolve sulfide ions. This observation is limited to sulfide capacity, and not sulfate capacity, because of the oxygen fugacities at which these prior geochemical studies were performed [25]. Most terrestrial magmas evolve under conditions in which Fe^{3+} and S^{2-} ions coexist [8 and 9], and thus over the range for which mutual interactions are observed.

High ferric contents result in increased supersulfide production according to equation (1). But at high S_2^- contents, reactions such as

$$S_2^- + S_2^- \rightleftharpoons S_4^{2-} \tag{4}$$

occur since tetrasulfide is a stable polysulfide ion [42, 45 and 47]. The chain length of this polysulfide ion increases by further polymerization to S_x^{2-}. Such reactions are consistent with the results that firstly more sulfur is incorporated in the melt than possible due to simple ferric ion oxidation, and secondly a sulfide-like ion must be formed. Polysulfides are, in fact, quite common in iron-rich melts [28]. Sulfides are thus very soluble in iron-rich melts due to these polysulfide ion formations, with the chain length of the polysulfide being a function of the composition and temperature [51]. These ions are unsaturated and have a high affinity for the excess Fe^{2+} ions in the melt as well as alkali ions.

5.5. Nuclear waste immobilization

Since iron and sulfur do not interact over a wide range of conditions in the reference system, prior models for redox constraints on the operation of a waste melter do not have to be appreciably modified [10 and 23]. A prior limit was the operation of the melter above an oxygen fugacity of 10^{-9} bar at 1150 °C in order to avoid sulfide or metal precipitation. Figures 6a to i show that appreciable sulfide may even be present at an oxygen fugacity of 10^{-8} bar in iron-rich melts because of the iron-sulfur interactions. However, this is still well within the prescribed processing range defined by an Fe^{2+}/Fe^{3+} ratio of 0.04 to 1.5 at 1150 °C [10]. Furthermore, the results indicate that in the iron-rich melts of nuclear waste systems, if the oxygen fugacity did indeed drift into the sulfide stability region, the capacity of the melt for sulfide ions is significantly greater than originally reported [2].

*

Support for this research was provided by the National Science Foundation (NSF: CPR-8406089), the Savannah River Laboratory, the Virginia Center for Innovative Technology, and the NSF-Industry-University Center for Glass Research at Alfred University.

6. References

[1] Plodinec, M. J.: Improved glass compositions for immobilization of SRP waste. In: Northrup, C. J. M. (ed.): Scientific basis for nuclear waste management 2. New York: Plenum Press 1980. p. 223–229.

[2] Schreiber, H. D.; Kozak, S. J.; Leonhard, P. G. et al.: Sulfur chemistry in a borosilicate melt. Pt. 1. Redox equilibria and solubility. Glastech. Ber. **60** (1987) no. 12, p. 389–398.

[3] Schreiber, H. D.; Kozak, S. J.; Leonhard, P. G. et al.: Sulfur chemistry in a borosilicate melt. Pt. 2. Kinetic properties. Glastech. Ber. **61** (1988) no. 1, p. 5–11.

[4] Schreiber, H. D.; Balazs, G. B.; Carpenter, B. E. et al.: An electromotive force series in a borosilicate glass-forming melt. J. Am. Ceram. Soc. **67** (1984) no. 6, p. C106–C108.

[5] Schreiber, H. D.; Leonhard, P. G.; Nofsinger, R. G. et al.: Oxidation-reduction chemistry of nonmetals in a reference borosilicate melt. In: Bickford, D. F. (ed.): Advances in the fusion of glass. Westerville, OH: Am. Ceram. Soc. 1988. p. 29.1–29.14.

[6] Schreiber, H. D.; Kozak, S. J.; Fritchman, A. L. et al.: Redox kinetics and oxygen diffusion in a borosilicate melt. Phys. Chem. Glasses **27** (1986) no. 4, p. 152–177.

[7] Schreiber, H. D.; Schreiber, C. W.; Leonhard, P. G. et al.: Solubility and diffusion of gases in a reference borosilicate melt. Diffusion & Defect Data **53–54** (1987) p. 345–350.

[8] Schreiber, H. D.: An electrochemical series of redox couples in silicate melts. A review and applications to geochemistry. J. Geophys. Res. **92** (1987) no. B9, p. 9225–9232.

[9] Schreiber, H. D.; Merkel, R. C.; Schreiber, V. L. et al.: Mutual interactions of redox couples via electron exchange in silicate melts. Models for geochemical melt systems. J. Geophys. Res. **92** (1987) no. B9, p. 9233–9245.

[10] Schreiber, H. D.; Hockman, A. L.: Redox chemistry in candidate glasses for nuclear waste immobilization. J. Am. Ceram. Soc. **70** (1987) no. 8, p. 591–594.

[11] Schreiber, H. D.; Kozak, S. J.; Balazs, G. B. et al.: Equilibrium and transport properties of gases in E-glass melts. J. Am. Ceram. Soc. **72** (1989) no. 9, p. 1680–1691.

[12] Goldman, D. S.: Redox and sulfur solubility in glass melts. In: Gas bubbles in glass. Prepared by Technical Committee 14 of the International Commission on Glass. Charleroi: Institut National du Verre 1985. p. 74–91.

[13] Bickford, D. F.; Diemer, R. B. jr.; Iverson, D. C.: Redox control of electric melters with complex feed compositions. Pt. 2. Preliminary limits for radioactive waste melters. J. Non-Cryst. Solids **84** (1986) no. 1–3, p. 285–291.

[14] Johnston, W. D.: Oxidation-reduction equilibria in iron-containing glass. J. Am. Ceram. Soc. **47** (1964) no. 4, p. 198–201.

[15] Goldman, D. S.: Oxidation equilibrium of iron in borosilicate glass. J. Am. Ceram. Soc. **66** (1983) no. 3, p. 205–209.

[16] Schreiber, H. D.; Carpenter, B. E.; Minnix, L. M. et al.: Precipitation of iron, cobalt, and nickel metal from a borosilicate glass melt. Glastech. Ber. **56K** (1983) Bd. 2, p. 1017–1022.

[17] Schreiber, H. D.; Kozak, S. J.; Merkel, R. C. et al.: Redox equilibria and kinetics of iron in a borosilicate glass-forming melt. J. Non-Cryst. Solids **84** (1986) no. 1–3, p. 186–195.

[18] Schreiber, H. D.; Minnix, L. M.; Balazs, G. B. et al.: The chemistry of uranium in borosilicate glasses. Pt. 4. The ferric-ferrous couple as a potential redox buffer for the uranium redox state distribution against oxidising agents in a borosilicate melt. Phys. Chem. Glasses **25** (1984) no. 1, p. 1–10.

[19] Schreiber, H. D.; Carpenter, B. E.; Eckenrode, J. P. et al.: The chemistry of uranium in borosilicate glasses. Pt. 5. The ferric-ferrous couple as a redox buffer for the uranium redox state distribution against reducing agents in a borosilicate melt. Phys. Chem. Glasses **26** (1985) no. 1, p. 24–30.

[20] Schreiber, H. D.: Redox processes in glass-forming melts. J. Non-Cryst. Solids **84** (1986) no. 1–3, p. 129–141.

[21] Bamford, C. R.: Colour generation and control in glass. Amsterdam, Oxford, New York: Elsevier 1977.

[22] Fanning, J. C.; Hunter, R. T.: Nuclear waste, glass, and the Fe^{2+}/Fe^{3+} ratio. J. Chem. Educ. **65** (1988) no. 10, p. 888–889.

[23] Bickford, D. F.; Diemer, R. B. jr.: Redox control of electric melters with complex feed compositions. Pt. 1. Analytical methods and models. J. Non-Cryst. Solids **84** (1986) no. 1–3, p. 276–284.

[24] Hlavac, J.: The technology of glass and ceramics. Amsterdam: Elsevier 1983.

[25] Katsura, T.; Nagashima, S.: Solubility of sulfur in some magmas at 1 atmosphere. Geochim. Cosmochim. Acta **38** (1984) p. 517–531.

[26] Haughton, D. R.; Roeder, P. L.; Skinner, B. J.: Solubility of sulfur in mafic magmas. Econ. Geol. **69** (1974) no. 4, p. 451–467.

[27] Carroll, M. R.; Rutherford, M. J.: Sulfide and sulfate saturation in hydrous silicate melts. Proc.15th Lunar Planet. Sci. Conf., J. Geophys. Res., Suppl. **90** (1985) p. C601–C612.

[28] Volf, M. B.: Chemical approach to glass. Amsterdam: Elsevier 1984.

[29] Zaman, M. S.; Paul, A.: A rapid method for the estimation of redox ions in iron-sulphur amber glasses. Glass Technol. **10** (1969) no. 4, p. 93–98.

[30] Close, W. P.; Tillman, J. F.: Chemical analysis of some elements in oxidation-reduction equilibria in silicate glasses. Glass Technol. **10** (1969) no. 5, p. 134–146.

[31] Weiser, S. M.: The effect of amber cullet additions on amber glass transmission. Ceram. Eng. Sci. Proc. **8** (1987) no. 3–4, p. 200–207.

[32] Paul, A.: Chemistry of glasses. London: Chapman & Hall 1982.

[33] Douglas, R. W.; Zaman, M. S.: The chromophore in iron-sulphur amber glasses. Phys. Chem. Glasses **10** (1969) no. 4, p. 125–132.

[34] Harding, F. L.: Effect of base glass composition on amber colour. Glass Technol. **13** (1972) no. 2, p. 43–49.

[35] Harding, F. L.; Ryder, R. J.: Amber colour in commercial silicate glasses. J. Can. Ceram. Soc. **39** (1970) p. 59–63.

[36] Loveridge, D.; Parke, S.: Electron spin resonance of Fe^{3+}, Mn^{2+}, and Cr^{3+} in glasses. Phys. Chem. Glasses **12** (1971) no. 1, p. 19–27.

[37] Mestdagh, M. M.; Dauby, C.; Van Cangh, L. et al.: Optical and electron paramagnetic resonance investigations of colour instabilities in amber glass as a function of melting temperature and batch redox conditions. Glass Technol. **24** (1983) no. 4, p. 184–191.

[38] Vogel, W.: Chemistry of glass. Westerville, OH: Am. Ceram. Soc. 1985.

[39] Presnell, D. C.; Brenner, N. L.: A method for studying iron silicate liquids under reducing conditions with negligible iron loss. Geochim. Cosmochim. Acta **38** (1974) p. 1785–1788.

[40] Sigel, G. H. jr.; Ginther, R. J.: The effect of iron on the ultraviolet absorption of high purity soda-silica glass. Glass Technol. **9** (1968) no. 3, p. 66–69.

[41] Jones, D. R.; Janskeski, W. C.; Goldman, D. S.: Spectrophotometric determination of reduced and total iron in glass with o-phenanthroline. Anal. Chem. **53** (1981) p. 923–924.

[42] Paul, A.; Ward, A.; Gomolka, S.: Origin of the blue colour in alkali borate glasses containing sulphur. J. Mater. Sci. **9** (1974) p. 1133–1138.

[43] Ahmed, A. A.; El-Shamy, T. M.; Sharaf, N. A.: Origin of blue and green colouration in sulphur containing alkali borate glasses. J. Non-Cryst. Solids **33** (1979) p. 159–167.

[44] Ahmed, A. A.; El-Shamy, T. M.; Sharaf, N. A.: States of sulfur in alkali borate glasses. J. Am. Ceram. Soc. **63** (1980) no. 9–10, p. 537–542.

[45] Giggenbach, W. F.: The blue solutions of sulfur in salt melts. Inorg. Chem. **10** (1971) no. 6, p. 1308–1310.

[46] Gruen, D. M.; McBeth, R. L.; Zielen, A. J.: Nature of sulfur species in fused salt solution. J. Am. Chem. Soc. **93** (1971) no. 24, p. 6691–6693.

[47] Giggenbach, W. F.: The blue supersulphide ion, S_2^-. J. Chem. Soc., Dalton (1973) p. 729–731.

[48] Seel, F.; Guttler, H. J.: Polysulfide radical ions. Angew. Chem. Internat. Ed. **12** (1973) no. 5, p. 420–421.

[49] Chivers, T.; Drummond, I.: Characterization of the trisulfur radical ion S_3^- in blue solutions and alkali polysulfides in hexamethylphosphoramide. Inorg. Chem. **11** (1972) no. 10, p. 2525–2527.

[50] Buchanon, D. L.; Nolan, J.: Solubility of sulfur and sulfide immiscibility in synthetic tholeiitic melts and their relevance to Bushveld complex rocks. Can. Mineral. **17** (1979) p. 483–494.

[51] Hanada, T.; Soga, N.; Kunugi, M.: Glass formation and structure of Na_2S-SiO_2 and $Na_2S-B_2O_3$ glasses. J. Non-Cryst. Solids **21** (1976) p. 65–72. 90R0275